

ANIMATING THE SEISMIC WAVEFIELD WITH USARRAY

Charles J. Ammon¹ and Thorne Lay²

¹Department of Geosciences, The Pennsylvania State University

²Department of Earth and Planetary Sciences, University of California, Santa Cruz

ABSTRACT

Seismic waves are continuous three-dimensional surfaces of associated ground motions that propagate through the Earth. Seismometers record the passage of numerous seismic waves through a given point near Earth's surface, and classically these seismograms are analyzed to deduce properties of the Earth's structure and the seismic source. Given a spatially dense set of seismic recordings, the signals can also be used to visualize the actual continuous seismic waves, providing new insights into complex wave propagation effects. Using signals recorded by an array of seismometers with unprecedented station density and aperture deployed as part of the NSF-funded EarthScope USArray project, we demonstrate innovative pedagogic and research applications of visualizations of the seismic wavefield.

INTRODUCTION: DENSE RECORDING OF SEISMIC WAVES ON A CONTINENTAL SCALE

Global seismologists have studied seismic wavefields for many years using sparse networks of isolated stations and/or relatively small aperture, narrow-band seismometer arrays. USArray, the primary seismological component of project EarthScope, will transform many aspects of conventional seismological analysis. USArray includes 400 broadband seismographs being deployed in the Transportable Array (TA), which will migrate across the United States over the next dozen years, occupying a total of 2000 sites for ~18 months each. The TA's primary scientific objective is to collect seismic

recordings over a continent-wide regularly spaced 70-km grid of sites to illuminate the underlying lithosphere and deeper mantle structure with unprecedented resolution. This project should revolutionize our understanding of the structure, evolution, and dynamics of North America in particular, and continents in general.

Many other applications of the TA seismic recordings will be possible due to the intrinsic multi-purpose nature of continuous, high dynamic range, broadband ground motion recordings, all of which are openly available by internet (<http://www.earthscope.org/>). These applications include quantification of the rupture process for large earthquakes around the world (Ammon et al., 2007), analyses of structure in the lower mantle and core of the Earth (van der Hilst et al., 2007) and in upper mantle regions remote from North America (Zheng et al., 2007), and detection and analysis of signals from regional earthquakes (e.g. Herrmann, 2007, Dreger, 2007) and exotic sources such as landslides, mine collapses (Ford et al., 2007), ocean storms (Rhie and Romanowicz, 2006), submarine slumps, volcanic eruptions, surging glaciers (Ekström et al., 2006), and large underground explosions (Ammon and Lay, 2006). The TA also enables a transformative view of the seismic wavefield, densely sampled over large spatial scale with high-quality seismometers. The dense sampling provides opportunities to visualize the ground motions as a wave phenomenon rather than focusing on point samples. This has previously only been viable for numerical models which compute complete wavefields, but now we can see actual Earth signals. This can help students of wave propagation on all levels to deepen their intuitive understanding of fundamental seismic-wave interactions, along with revealing complexities that cannot be recognized in individual seismograms.

The TA stations have uniform installation procedures and well-calibrated instrument responses that produce high-fidelity recordings of the seismic wavefield over an area with dimensions of about 1500 x 1000 km. The first full deployment of all 400 TA stations has now been completed across the western United States, covering California, Oregon, Washington, Arizona, Utah, and Idaho. The high quality of the observations is illustrated using a traditional seismic record section in Figure 1, showing individual seismograms at different distances from the source. The section shows vertical-component displacement seismograms from the great 12 September 2007 Sumatra earthquake (M_w 8.4). Both body waves (P and S, and their multiple reflections from the surface and core) and dispersed Rayleigh waves in the teleseismic wavefield are present and can be tracked from trace to trace. The long source rupture process of this event (which had a duration of about 80 seconds) enhances the low-frequency content of the signals. Such record sections are the conventional display of seismic vibrations, effectively conveying travel times of specific wave types as a function of propagation distance. However, the spatial/temporal aspects of the wavefield are not fully revealed, and our objective is to use these dense TA recordings to image the waves associated with these motions.

Ground-Displacement Animations

We consider animations of the waves at the TA stations that capture the spatial and temporal behavior of the ground motions for both expected and unexpected wave interactions with geologic structures beneath the western North America. QuickTime animations are available on-line at <http://eqseis.geosc.psu.edu/~cammon/QA/> Two still frames from an animation of the great April 2007 Solomon Islands earthquake are shown

in Figure 2. In both panels, each circle represents a TA station for which ground motions were recorded and the gray arrow shows the expected direction of wave travel if the Earth is radially symmetric. Time values, shown to the lower left, are referenced to the event origin time. The frame in Figure 2a shows a snapshot of ground motions during the propagation of direct S waves arrivals sweeping across the western U. S.; Figure 2b shows the propagation of Rayleigh wave arrivals (R2) that sweep across the western U.S. almost two hours later having traveled on the long-arc of the great-circle containing the source and stations, and hence arriving from the southeast. Symbol color indicates the amplitude of ground displacement at this particular snapshot in time (blue is downward motion, red is upward motion). For the animation, the displacement seismograms were corrected for a gain factor and band-pass filtered to include signals with periods between 250s and 50s.

When you view the movies, you will see the progressive passage of wave after wave across the array primarily sweeping one way or another along the great-circle direction. The full space-time evolution of the wavefield is revealed, recapturing much of the essence of the wave phenomena suppressed in the seismic profile in Figure 1. The wavelengths of the propagating signals are directly revealed, as are the geometries and irregularities of the wavefronts produced by 3-dimensional heterogeneity along the path. The QuickTime animations allow one to sweep the wavefield back and forth, evaluating in detail how the ground motions evolve over time. Our experience in the classroom suggests that students more immediately grasp the nature of the time variations when the spatial evolution of the waves is displayed compared to what they glean from seismic profiles. It is straightforward to design exercises that involve measurement of

wavelength, phase velocity, and overlapping wave interference, all of which are intuitively conveyed by the visualizations. Numerical simulations can be similarly visualized and compared with the data.

Normal Modes

Very large earthquakes excite long-period standing-wave vibrations throughout the planet that are detectable for weeks following the event. In the early hours after the energy release occurs these vibrations can best be thought of and analyzed as propagating waves spreading throughout the planet or traveling along the surface. At later times, the deformations have extensively interacted, beating against each other to produce patterns of constructive and destructive interference, which are more clearly viewed as standing oscillations like those associated with a ringing bell (e.g. Lay and Wallace, 1995; Stein and Wysession, 2003).

To visualize the western U.S. ground movement associated with Earth's "normal modes", we extracted about 12 hours of ground motions beginning about 37 hours after the 12 September, 2007 Sumatra earthquake. Two frames from the animation during this time interval are shown in Figure 3. The frames show the pattern of alternating uplift and downwarping of the entire western US as a result of Earth's normal mode deformations. The period of the specific oscillation shown is about 700 s (~12 minutes). A viewing of the animation shows that the overall pattern of continental motions is much more complicated than a simple, slow up and down motion, as a result of multiple overlapping modes beating simultaneously. To our knowledge, this is the first spatially-resolved display of true normal modes in action for the Earth. Corresponding patterns of surface motions on the Sun observed by Doppler velocity field measurements of the surface have

long been analyzed in the field of helioseismology to constrain internal structure of the star (e.g., Harvey, 1995). If you watch the full animation closely, you'll see propagating waves from the 14 September 2007 06:01:34 Ms 6.4 aftershock sweep across the array. Again, simulations can be similarly animated to demonstrate predictability of the observed beating patterns.

Long-Period Scattered Rayleigh Waves

The animations discussed above and available on the web are dominated by wave phenomena that are expected and predictable with existing Earth models and computational procedures. But one of the advantages of the animations is that they can reveal subtle anomalies in the wave patterns that might otherwise go unrecognized. This is partly because it is straightforward to see waves that sweep across the array with directions other than along the great-circle path. Such waves can arise either from superimposed signals from multiple sources in different locations, or from scattering of waves from a given source that results in waves traveling on different paths. Since spatially separated earthquakes can be individually located even if they are closely spaced in time, we can distinguish between these possibilities.

Several examples of scattered arrivals, are apparent in the on-line animations. Figure 4 shows a snapshot of a time interval following the April 2007 great Solomon Islands earthquake where a wavefront sweeps across the array with a trajectory at large angles to the great-circle path along which the expected wavefronts propagate. Standard array processing procedures, applied to the continental scale TA can quantify these late anomalous phases. From the arrival time of the anomalous waves, their periods, as well as direct measurement of their propagation direction and phase velocity (Figure 4), we

can associate the scattered waves with scattered surface waves that originate in the northwest Pacific subduction zones. Observations like these can be used to constrain three-dimensional heterogeneities in the mantle; in the Solomon Islands case the likely cause is associated with subducting slab structure or ocean/continent lateral transition gradients. Out-of-great-circle scattered arrivals are also clearly seen for the 15 August 2007 Peru earthquake and the 15 October 2006 Hawaii earthquake animations. We find that scattering varies with event location, indicating that the combined effects of source radiation and geometry relative to the scattering structure influence the strength of the scattered arrivals.

Accessing the Animations

The ground motion animations for TA recordings are provided on-line for seven of the largest recent earthquakes. These animations provide a new view of wave interactions, including examples of amplitude focusing and effects of heterogeneity on the deterministic components of the wavefield. The animations are a valuable guide for global seismological research, such as the analysis of long-period surface-wave scattering illustrated above, as well as for correlating earthquake triggering with seismic wave passage. In addition, the seismic wavefield animations are extremely effective in educational presentations. At the introductory non-science level, all students can quickly appreciate some basic ideas related to earthquake location, such as the direction to the earthquake. In more quantitative classes, students can use the animations side-by-side with more traditional seismogram plots and record sections to study fundamental concepts such as phase velocity, wavelength, scattering, etc. Using familiar computer tools such as QuickTime Player, students can explore the propagating waves using

sliders, running the animations backwards and forwards at their preferred speed, exploring seismic wave propagation phenomena at their own pace.

More animations will be routinely prepared and made openly available for future large earthquakes as they occur (from the Incorporated Research Institution for Seismology website at <http://www.iris.edu/>). With the TA progressively migrating eastward across the conterminous states, and then on to Alaska there will be many new views of the seismic wavefield for a host of geometries.

Acknowledgements. This work was supported in part by the U.S. National Science Foundation under EarthScope grant EAR-0453884 (TL) and the U.S. Geological Survey under award number 05HQGR0174 (CJA). USArray is supported by NSF as part of the EarthScope project under Cooperative Support Agreement EAR-0323309.

References

- Ammon, C. J., and T. Lay (2007), Nuclear test illuminates USArray data quality, *EOS, Trans. Am. Geophys. Union*, **88**, 37-38.
- Ammon, C. J., H. Kanamori, and T. Lay (2007). A great earthquake doublet and seismic stress transfer cycles in the Central Kuril Islands, *Nature*, submitted.
- Dreger, D., UC Berkeley Moment Tensor Catalog, <http://seismo.berkeley.edu/~dreger/mtindex.html>, 2007.
- Ekström, G., M. Nettles, and V. C. Tsai (2006), Seasonality and increasing frequency of Greenland glacial earthquakes, *Science*, **311**, 1756-1758.
- Ford, A, Seismic Moment Tensor Report for the 06 Aug 2007, M3.9 Seismic event in central Utah, <http://seismo.berkeley.edu/~peggy/Utah20070806.htm>, 2007.
- Harvey, J. (1995), Sounding out the Sun, *Physics Today*, October, 32-38.

- Herrmann, R. B., Focal mechanism determinations for US,
http://www.eas.slu.edu/Earthquake_Center/MECH.NA/index.html, 2007.
- Lay, T., and T. C. Wallace (1995), *Modern Global Seismology*, 517 pp., Academic Press, New York.
- Rhie, J., and B. Romanowicz (2006) A study of the relation between ocean storms and the Earth's hum, *Geochem., Geophys. Geosys.* **7**, Q10004, doi:10.1029/2006GC001274.
- Stein, S., and M. E. Wysession (2003), *An Introduction to Seismology, Earthquakes, and Earth Structure*, 498 pp., Blackwell, Malden, MA.
- van der Hilst, R. D., M. V. deHoop, P. Wang, S.-H. Shim, P. Ma, and L. Tenorio (2007), Seismostratigraphy and thermal structure of Earth's core-mantle boundary region, *Science*, **315**, 1813-1817.
- Zheng, Y., T. Lay, M. P. Flanagan, and Q. Williams (2007). Pervasive seismic wave reflectivity and metasomatism of the Tonga mantle wedge, *Science*, **316**, 855-859.

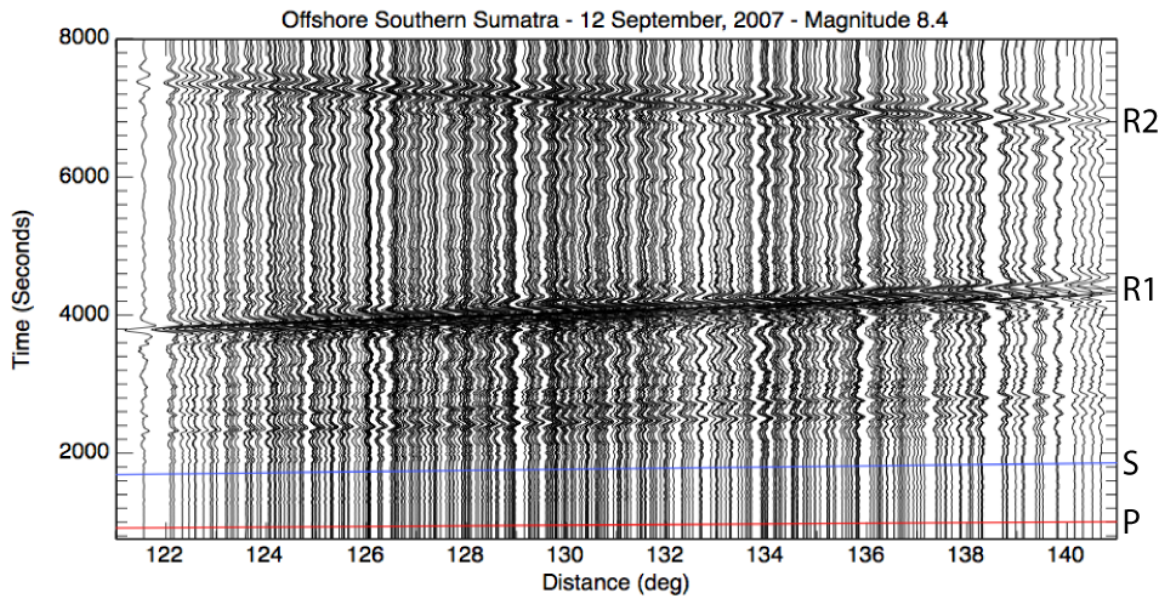


Figure 1. A traditional seismic record section showing the consistency of observations across the large-aperture TA. Theoretical iasp91 arrival times are indicated (the event had a rupture duration of roughly a minute). The short-arc arrivals (P, S, R1) travel the shorter distance from the source to the array; the longer arc arrivals (R2) leave the source region and travel the long-wave around the planet.

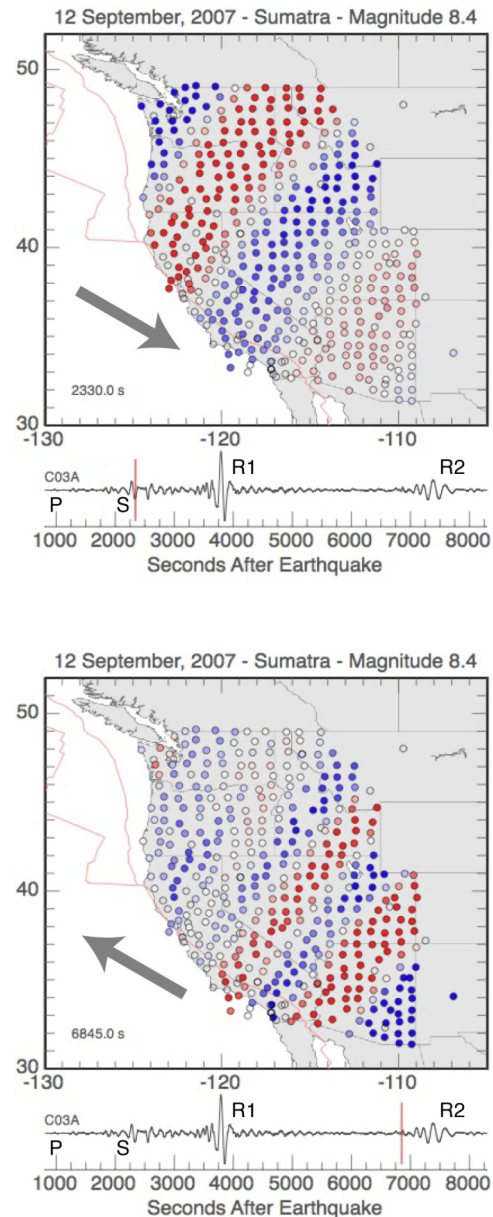


Figure 2 Snapshot of ground motion during the passage of the seismic waves across western North America. Blue regions show downward displacements and red symbols indicate upward displacements. The predicted direction of wave motion is indicated by the gray arrow. (Top) The alternating blue and red regions show large amplitude S-wave motion about 2,330 seconds (~39 minutes) after the event origin. (Bottom) Snapshot of ground motion during the passage of the long-arc Rayleigh wave. The great distance from the earthquake to the array results in a nearly planar wavefronts.

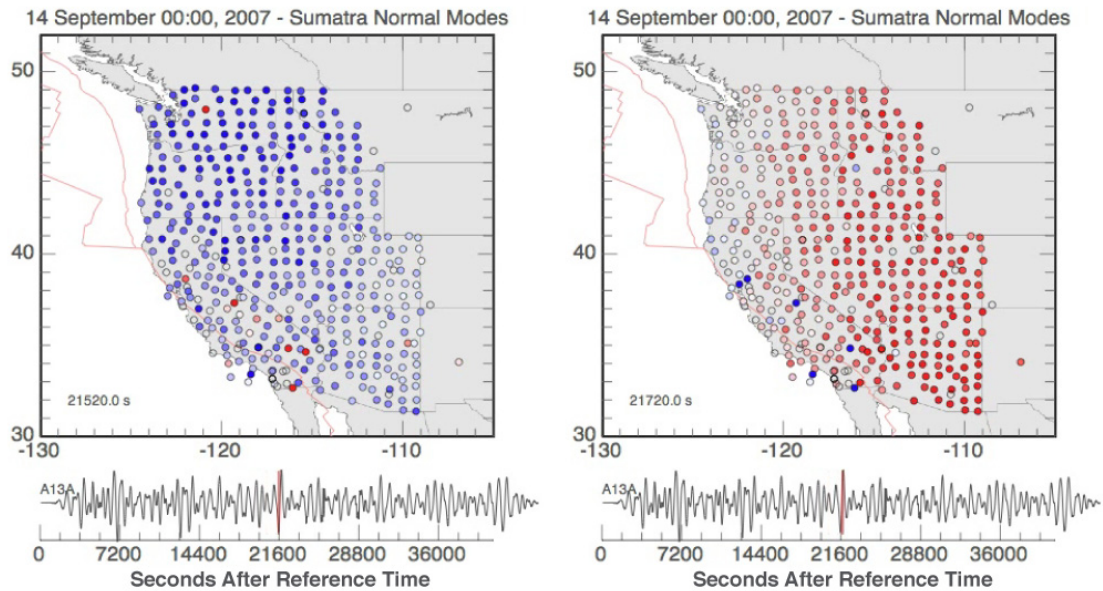


Figure 3. Snapshots of ground motion during normal-mode induced deformation roughly 43 hours following the earthquake (the reference time is shown in the frame title). The amplitudes shown here are about 1000 times smaller than those shown in Figure 2. The image on the left shows a time when most of the western United States were below their nominal level; about 3 minutes later, the ground had moved upward past the nominal ground elevations. Stations not matching the overall pattern are those that contain noise glitches.

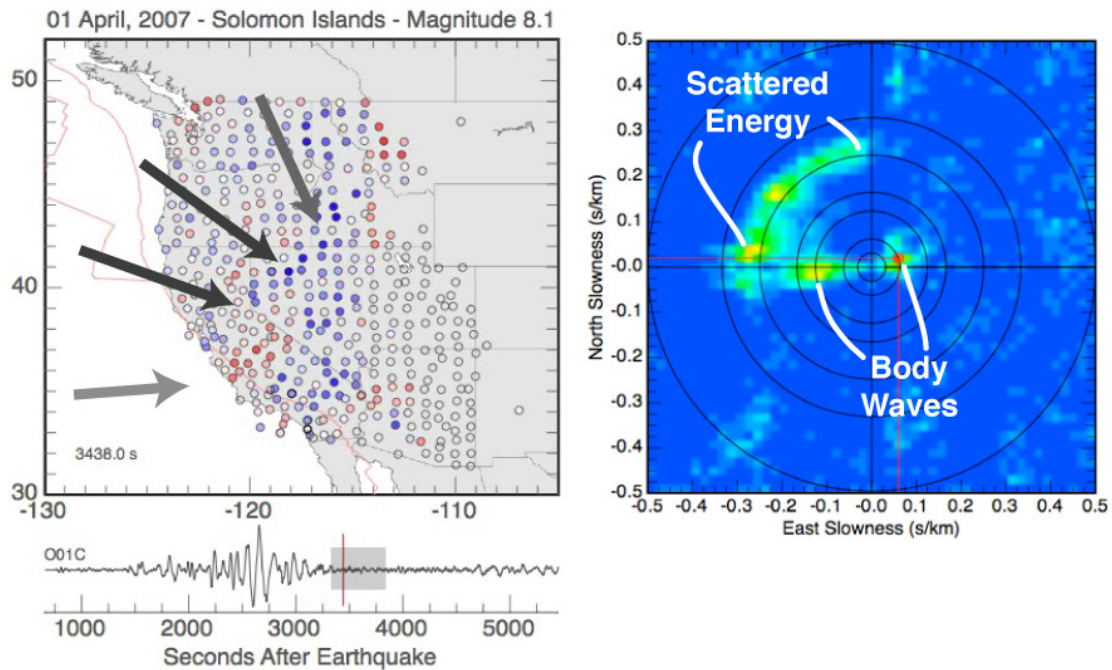


Figure 4. Snapshot of scattered waves observable in the R1 coda. The arrivals are not clear in a single frame, but the animation clearly shows propagation of waves well away from the expected direction (the light gray arrow). The image on the right is a slowness spectrum computed for a time centered on the frame (gray box on the seismogram). The slowness spectrum allows us to estimate the direction of wave propagation, and the phase velocity of the wave (given by the distance from the plot origin). This time window is rich in arrivals, including two waves with body-wave slowness, and a swath of energy arriving from the northwest with surface-wave slownesses.